

Stability and Delay Analysis of Multi-Link Slotted Aloha with Cloning Strategy

Buwei Wu*, Wen Zhan*, Xinghua Sun*, Minjie Liu* and Yue Zhang[†]

*School of Electronics and Communication Engineering, Shenzhen Campus of Sun Yat-sen University, China

[†]Department of Electronic and Information Engineering, Shantou University, China

wubw7@mail2.sysu.edu.cn, {zhanw6, sunxinghua}@mail.sysu.edu.cn, liumj78@mail2.sysu.edu.cn, yuezhang@stu.edu.cn

Abstract—In the emergent landscape of next-generation communication networks, multi-link operation is becoming significant for random access protocols owing to its potent multi-stream concurrent transmission capabilities. Yet, in the context of random access networks, the intricate coupling relationships among links make the stability analysis tricky. This paper considers the stability property of a multi-link slotted Aloha system, where the Cloning strategy is considered that sets up devices to transmit identical data replicas over separate links. By analyzing the state transition process of the head-of-line packet of each multi-link device, we identify distinct steady-state points and delineate the boundaries of stability regions for each link under various traffic conditions. Iterative algorithms are proposed to determine the network stability situation and the effectiveness is verified via simulation results on network access delay performance.

Index Terms—Multi-Link, slotted Aloha, stability region, performance analysis.

I. INTRODUCTION

The exponential growth of IoT technology has presented next-generation wireless communication networks with opportunities and challenges that were previously unanticipated. The exponential growth of connection density among Internet of Things (IoT) devices has been attributed to the ascent and realization of the concept of massive Machine-Type Communication (mMTC). This exponential increase poses a serious challenge for conventional multiple-access technologies. Contention-based random access techniques have progressively emerged as a pivotal resolution to the machine-type communication dilemma within this particular context. The slotted Aloha scheme, however, as a typical type of random access, has been put to a more rigorous test due to the escalating quality of service (QoS) requirements in the emerging vertical application areas. Research shows that slotted Aloha networks' average access delay exceeds hundreds of time slots [1], which fails IoT wireless communication requirements.

This work was supported in part by The Shenzhen Science and Technology Program (No.RCBS20210706092408010), in part by Open Fund of State Key Laboratory of Satellite Navigation System and Equipment Technology (No. CEPNT-2021KF-04), in part by the Science and Technology Planning Project of Key Laboratory of Advanced IntelliSense Technology, Guangdong Science and Technology Department under Grant 2023B1212060024, in part by Guangdong Basic and Applied Basic Research Foundation (No. 2024A1515012015), in part by the National Natural Science Foundation of China under Grant 62201336, in part by Guangdong Natural Science Foundation under Grant 2024A1515011541, and in part by the STU Scientific Research Initiation Grant (SRIG) of Shantou University under Grant NTF 21039.

This has also reduced its application potential. How to more efficiently utilize the limited transmission resources to meet the rising QoS demand has become an imperative matter that must be resolved expeditiously for the slotted Aloha scheme.

In this regard, the next-generation IEEE 802.11be standard introduces multi-link operation (MLO), paving the way for further advancements in wireless communication. Multi-link devices (MLD) that combine multiple radios into one unit have the superior ability to transmit simultaneously over various links, leading to extremely high data transmission capacity with low latency performance. This improvement has been widely witnessed in existing studies on the performance analysis of Wi-Fi networks with multi-link operation [2]–[4]. It is conceivable that, for IoT scenarios, the multi-link operation would be an intriguing and promising option for wireless communication networks to satisfy the expanding QoS requirements in numerous applications.

Even though MLO is a nascent technological advancement, Aloha networks have implemented the notion of multi-channel transmission for a sizable duration. As in multi-channel Aloha networks, diverse channel-hopping or channel selection schemes have been proposed for devices to choose one channel for data transmission [5], [6], however miss out on the diversity gain when multiple channels are accessible if the devices are equipped with multiple radios [7], [8]. To the best of our knowledge, how to model and analyze the stability of the multi-link slotted Aloha networks is still an open issue. The challenge lies in characterizing the intrinsic relation between the data queue, as well as the multiple links inside each MLD and the coupling effect among MLDs due to the contention on channels.

To characterize the mean access delay performance through multi-link operation, nevertheless, the stability analysis of the slotted Aloha network must take precedence. Extensive research has been conducted on the stability analysis of slotted Aloha network [9]–[11], where the key lies in modeling the mutual coupling effect between the data queues of the nodes, as each node's successful transmission requires other nodes to remain mute. The analysis is challenging due to the inherent bi-stable behavior problem in Aloha networks. That is, the network has two steady-state points (i.e., the successful transmission probabilities of packets) and suffers the risk of dropping to the lower one, on which the network performance becomes poor. How to analyze the stability of the multi-link

slotted Aloha networks remains an open but important issue.

This paper addresses the above open issues by focusing on the multi-link slotted Aloha networks with *Cloning* strategy [12], that is, the device sends full copies of each packet through different links. The packet transmission is successful if at least one copy is successfully decoded. In each channel, there is an external network that resides and joins the channel contention with Poisson-distributed traffic arrivals. Our analysis starts by establishing a discrete-time Markov model for characterizing the behavior of the Head-of-Line (HoL) packet of each MLD, where the intrinsic relation between the successful deliveries of HoL packets among different links is included based on the *Cloning* strategy. Steady-state points in each channel are derived and calculated based on an iterative algorithm. Furthermore, we study the stability properties of the multi-link Aloha network and obtain explicit expressions of the boundaries between the all-saturated/queue-stable regions on different links, and propose an iterative algorithm to determine whether the MLDs are saturated or not. The latency performance of the MLDs has been discussed.

The remainder of this paper is organized as follows. The system model is presented in Section II, while both the service rates of the MLDs' data queues and the steady-state points of each link are addressed in Section III. Section IV presents the stability regions analysis. The Mean access delay performance is analyzed in Section V. Concluding remarks are summarized in Section VI.

II. SYSTEM MODEL

Consider a heterogeneous time-slotted random access network with L channels, consisting of one multi-link group and L external group, as illustrated in Fig. 1. The multi-link group is referred to as Group M , a collection of n MLDs, wherein each MLD has the ability to independently transmit data across all L channels. The buffer size of each MLD is infinite and the packet arrival process at each MLD follows a Bernoulli distribution with parameter $\lambda \in [0, 1]$. Each MLD with a non-empty buffer would transmit packets in channel c with probability $q^{(c)} \in [0, 1]$ and $\mathbf{q} = (q^{(1)}, \dots, q^{(L)})$ is the random access strategy vector for each MLD. \mathbf{q} may vary from channel to channel, such that the MLD may maintain silence on certain channels while transmitting on others.

Note that random access networks, such as Wifi and Bluetooth, usually operate in the ISM (Industrial Scientific Medical) band and encounter complex while unknown radio interference. To model external interference, we assume in each channel, an external network resides, denoted as network $c \in \{1, \dots, L\}$, and join the channel contention with the multi-link group. Similar to [13], here we presume that the total number of channel attempts generated by both fresh and backlogged packets from the external network c in each time slot follows the Poisson distribution with the parameter G_c without loss of generality, and $\mathbf{G} = (G_1, \dots, G_L)$. Assume that every packet transmission and additional processes (including acknowledgment and access initiation) are limited to a single time slot. The packet can be successfully decoded in the absence of concurrent transmissions. Otherwise, a collision occurs and all packet transmissions fail.

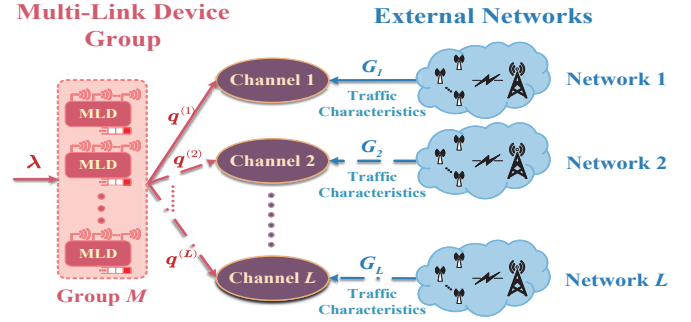


Fig. 1. The network comprises an individual coexistence of L transmission channels. The Multi-Link device group M is composed of n MLDs. The traffic characteristics of channel c are impacted by transmission requests from network c ($\forall c \in \{1, \dots, L\}$).

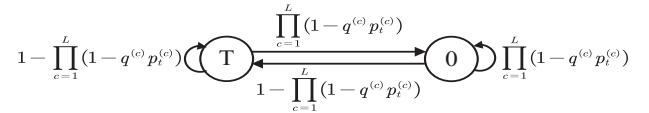


Fig. 2. State transition diagram of each HoL packet from Group M while transmitting on all L channels.

To improve the reliability, each MLD adopts *Cloning* strategy [12]. The packet transmission is successful as long as one copy in any channel is successfully decoded at the receiver. It is clear that the service rate of an MLD's queue depends on the behavior of other MLDs and external networks. Even with the *Cloning* strategy, it is possible the channel contention becomes severe if the traffic input rates are large or the transmission probabilities are selected improperly, causing the number of packets in each MLD's queue to grow unboundedly with time, in which case the MLD group becomes unstable. Given any system configuration, how to determine the stability of the MLD group is the key issue that we will address in this paper.

III. MODELING AND STEADY-STATE POINT ANALYSIS

Denote the successful transmission probability of channel c for each packet at time slot t as $p_t^{(c)}$, and the steady-state point (the limiting probability of successful transmission) of channel c as $p^{(c)}$, where $c \in \{1, \dots, L\}$. The behavior of the Head-of-Line (HoL) packet of each MLD can be characterized based on the discrete-time Markov process established in [9], where State T denotes the successful transmission state and State 0 denotes the waiting state. As Fig. 2 shows, a fresh HoL packet is initially in State T and moves back to State T if it is successfully transmitted. When the transmission fails, the HoL packet moves and stays in State 0, until it is successfully transmitted and then moves back to State T .

The steady-state probability distribution of the Markov chain in Fig. 2 can be given by

$$\begin{cases} \pi_T = 1 - \prod_{c=1}^L (1 - q^{(c)} p^{(c)}), \\ \pi_0 = \prod_{c=1}^L (1 - q^{(c)} p^{(c)}). \end{cases} \quad (1)$$

Note that $p^{(c)} = \lim_{t \rightarrow \infty} p_t^{(c)}$ is the steady-state probability of successful transmission of channel c for the MLDs' HoL packets and π_T is the service rate of each MLD's data queue.

It should be pointed out that in each channel, whether the packet transmission is successful or not is independent of the concurrent transmissions from both the external networks and

MLDs in other channels. Regarding this, we can simplify the steady-state point analysis by focusing on one randomly selected channel, e.g., channel c . In channel $c \in \{1, \dots, L\}$, for any device of Group M , the packet transmission is successful if and only if all other devices from Group M are either idle or loaded but not requesting transmission, as well as no other requests from the external network c .

Let p_{emp} denotes the probability that the data queue of an MLD is empty and $K^{(c)}$ the number of channel requests from external network c . The successful transmission probability of the HoL packet of each MLD's data queue, i.e., $p^{(c)}$, in channel c can be written as

$$p^{(c)} = \Pr\{K^{(c)} = 0\} \left(p_{emp} + (1 - p_{emp})(1 - q^{(c)}) \right)^{n-1} \quad (2)$$

where $\Pr\{K^{(c)} = k\} = \frac{(G_c)^k}{k!} e^{-G_c}$, $k = \{0, 1, \dots\}$.

For each MLD, the probability that the queue is empty, i.e., p_{emp} , depends on the service rate and the traffic input rate. Specifically, if the traffic input rate λ is smaller than its service rate π_T , then the queue is non-empty with the probability $\frac{\lambda}{\pi_T}$; Otherwise, the queue length would grow without a bound and the queue is saturated with $p_{emp} = 0$, i.e., [9]

$$p_{emp} = \begin{cases} 1 - \frac{\lambda}{\pi_T}, & \lambda < \pi_T \\ 0, & \lambda \geq \pi_T. \end{cases} \quad (3)$$

Equations (2)–(3) reveal that the stability of the data queue crucially determines the steady-state point in each channel. Thus, it is necessary to discuss the steady-state point $p^{(c)}$ in two different cases: Group M is saturated or unsaturated.

1) When Group M is saturated, i.e., $p_{emp} = 0$, the steady-state point $p_S^{(c)}$ is given by

$$p_S^{(c)} = e^{-G_c} (1 - q^{(c)})^{n-1} \approx \exp(-G_c - nq^{(c)}), \quad (4)$$

with approximation $(1 - x)^a \approx \exp(-ax)$ when x is small and n is large. Similar to [9], here we refer to $p_S^{(c)}$ as the undesired steady-state point.

2) When Group M is unsaturated and $\lambda < \pi_T$, the steady-state point $p_U^{(c)}$ is given by

$$p_U^{(c)} \approx \exp \left[-G_c - \frac{n\lambda q^{(c)}}{1 - \prod_{i=1}^L (1 - q^{(i)} p_U^{(i)})} \right], \quad (5)$$

which is jointly determined by all the steady-state points from all the channels. It can be shown that the above fixed-point equation has two non-zero roots, denoted by $p_{U,L}^{(c)}$ and $p_{U,S}^{(c)}$, where $p_{U,L}^{(c)} \geq p_{U,S}^{(c)}$ [9], and only the larger root $p_{U,L}^{(c)}$ is the steady-state point.

We can observe from (4) and (5) that only in the unsaturated case, the steady-state point $p_{U,L}^{(c)}$ depends on the steady-state points of other channels, implying tight coupling effect among the behavior of MLDs in different channels. In particular, the relationship between the steady-state points in any two different channels, denoted by $p_{U,L}^{(i)}$ and $p_{U,L}^{(j)}$, can be demonstrated through the following equation

$$p_{U,L}^{(j)} = \exp \left[\frac{q^{(j)}}{q^{(i)}} (\ln p_{U,L}^{(i)} + G_i) - G_j \right], \quad (6)$$

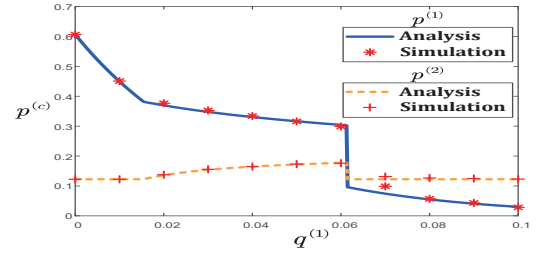


Fig. 3. Steady-state points $p^{(1)}$ and $p^{(2)}$ versus the transmission probability on channel 1, i.e., $q^{(1)}$. $L = 2$, $n = 30$, $\lambda = 0.25/n$, $G_1 = 0.5$, $G_2 = 1.5$, $q^{(2)} = 0.02$.

Algorithm 1: Calculation of steady-state points in the unsaturated case

Input: n , λ , L , $\mathbf{G} = (G_1, \dots, G_L)$,

$\mathbf{q} = (q^{(1)}, \dots, q^{(L)})$ and ϵ .

Output: $\mathbf{P}_U = (p_{U,L}^{(1)}, p_{U,L}^{(2)}, \dots, p_{U,L}^{(L)})$

- 1 Initiate $F = 1$, $p^{(1)} = 1$.
- 2 **while** $F > 0$ **do**
- 3 $p_{U,L}^{(1)} = p_{U,L}^{(1)} \times \epsilon$;
- 4 Calculate $F(p_{U,L}^{(1)})$ according to Eq. (7) ;
- 5 **end**
- 6 Calculate the remaining $p_{U,L}^{(c)}$, $\forall c \in \{2, \dots, L\}$ according to (6).

where $\forall i, j \in \{1, \dots, L\}$ and $i \neq j$. Based on (5) and (6), an iteration-based Algorithm 1 is proposed to derive $\mathbf{P}_U = (p_{U,L}^{(1)}, \dots, p_{U,L}^{(L)})$ in the Multi-Link network when all MLDs operate in the unsaturated status. The basic idea of Algorithm 1 starts with

$$F(p_{U,L}^{(c)}) = \frac{n\lambda q^{(c)}}{G_c + \ln p_{U,L}^{(c)}} + 1 - \prod_{i=1}^L [1 - p_{U,L}^{(i)} * q^{(i)}], \quad (7)$$

where (7) has the same non-zero roots as (5). Combining (6), all $p_{U,L}^{(i)}$ can be calculated by approximating $F(p_{U,L}^{(c)}) \rightarrow 0$ with step size $\epsilon \in (0, 1)$.

Fig. 3 demonstrates how the steady-state point $q^{(c)}$ ($c \in \{1, \dots, L\}$) varies with the MLDs' transmission probability on channel 1, $q^{(1)}$, when $L = 2$. Although the packet decoding on different channels is independent, the steady-state point on channel 2, $p^{(2)}$, arises when $q^{(1)}$ increases. Intuitively, in the unsaturated status, a larger $q^{(1)}$ leads to higher service rates of the data queues, where the HoL packets can be successfully transmitted through channel 1 and therefore the contention in channel 2 is relieved. The simulation results reveal the coupling effect among different channels and also verify the steady-state point analysis.

IV. STABLE REGION

So far, we have derived the steady-state points of each channel given the MLD group is saturated or unsaturated. This section will further address how to determine whether the MLD group is saturated or not.

Similar to [9], we can define the stability regions as follows:

- **Queue-stable Region** $\mathcal{S}_Q = \{(n, \lambda, \mathbf{q}, \mathbf{G}) | \lambda < \pi_T\}$, within which Group M operates in the unsaturated status.

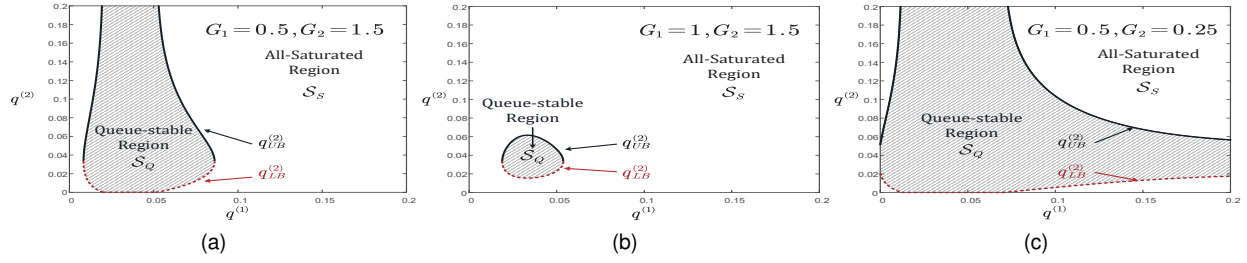


Fig. 4. Queue-stable region \mathcal{S}_Q and All-saturated region \mathcal{S}_S versus the transmission probability on each channel $q^{(c)}$ with (a) $G_1 = 0.5, G_2 = 1.5$, (b) $G_1 = 1, G_2 = 1.5$ and (c) $G_1 = 0.5, G_2 = 0.25$, where $L = 2$ and $c \in \{1, 2\}$, $n = 30$, $\lambda = 0.2/n$.

Theorem 1. Given the group size n , the traffic input rate λ , the channel access attempt rates of the external networks \mathbf{G} and the transmission probabilities $\mathbf{q} \setminus q^{(c)}$, if $q^{(c)} \in [q_{LB}^{(c)}, q_{UB}^{(c)}]$, then Group M operates in the Queue-stable region \mathcal{S}_Q . Otherwise, Group M operates in the All-saturated region \mathcal{S}_S , where

$$q_{LB}^{(c)} = \begin{cases} 0, & \text{if } \lambda \leq \lambda_q^{(c)} \\ -\frac{1}{n} \mathbb{W}_0 \left[\frac{ne^{G_c}(1-\lambda)}{\prod_{i \in L \setminus c} (1-q^{(i)} \exp(-nq^{(i)} - G_i))} - ne^{G_c} \right], & \text{otherwise,} \end{cases} \quad (8)$$

and

$$q_{UB}^{(c)} = \begin{cases} 1, & \text{if } \lambda \leq \lambda_q^{(c)} \\ -\frac{1}{n} \mathbb{W}_{-1} \left[\frac{ne^{G_c}(1-\lambda)}{\prod_{i \in L \setminus c} (1-q^{(i)} \exp(-nq^{(i)} - G_i))} - ne^{G_c} \right], & \text{otherwise,} \end{cases} \quad (9)$$

where $\mathbb{W}_0(\cdot)$ and $\mathbb{W}_{-1}(\cdot)$ are two branches of the Lambert W function and

$$\lambda_q^{(c)} = 1 - [1 - \exp(-n - G_c)] \prod_{i \in L \setminus c} [1 - q^{(i)} \exp(-nq^{(i)} - G_i)], \quad (10)$$

if and only if the traffic input rate λ satisfies

$$\lambda < \lambda_B^{(c)} = 1 - \left[1 - \frac{\exp(-G_c)}{ne} \right] \prod_{i \in L \setminus c} [1 - q^{(i)} \exp(-nq^{(i)} - G_i)]. \quad (11)$$

Proof: See Appendix A. ■

- **All-saturated Region** $\mathcal{S}_S = \overline{\mathcal{S}_Q}$ is the complementary set of \mathcal{S}_Q and Group M operates in the saturated status.

Lemma 1 presents the necessary but insufficient condition that Group M operates in the Queue-stable region \mathcal{S}_Q .

Lemma 1. The necessary but insufficient condition that Group M operates in the Queue-stable region \mathcal{S}_Q is $\lambda < \lambda_{\max}$, where

$$\lambda_{\max} = 1 - \prod_{c=1}^L \left[1 - \frac{\exp(-1 - G_c)}{n} \right]. \quad (12)$$

Otherwise, Group M operates in the All-saturated region \mathcal{S}_S regardless of \mathbf{q} .

Proof: Taking the first-order and second-order derivatives of (4), the Hessian matrix of π_T with respect to the stationary point $q^* = (\frac{1}{n}, \dots, \frac{1}{n})$ can be derived and we can subsequently prove that the stationary point q^* is the maximum point of the service rate π_T and derive λ_{\max} . ■

Lemma 1 is intuitively clear. That is, if the traffic input rate is too large and exceeds the maximum service rate that the network can provide, then the number of packets in the buffer grows with time regardless of access control strategy. On the other hand, if the traffic input rate is small, then whether Group

M is saturated or not crucially depends on the transmission probabilities vector $\mathbf{q} = (q^{(1)}, \dots, q^{(L)})$.

As stable regions are high dimensional spaces with multi-variables, characterizing the explicit expressions of the Queue-stable region \mathcal{S}_Q and the All-saturated region \mathcal{S}_S is difficult. Accordingly, in this paper, we aim to address how to determine whether the MLD group is saturated or not given the group size n , the traffic input rate λ , the transmission probabilities \mathbf{q} and the access attempt rates of the external networks \mathbf{G} based on Algorithm 2, for which the key lies in Theorem 1.

Specifically, given the transmission probabilities of all other channels $\mathbf{q} \setminus q^{(c)}$, if the transmission probability in channel c , $q^{(c)} \in [q_{LB}^{(c)}, q_{UB}^{(c)}]$, then Group M operates in the Queue-stable region \mathcal{S}_Q . Otherwise, it is in the All-saturated region \mathcal{S}_S , where $q_{LB}^{(c)}$ and $q_{UB}^{(c)}$ are given in Theorem 1. Therefore, the basic idea of Algorithm 2 is that by repeatedly applying Theorem 1 on each channel, the saturation condition of Group M can be determined on any given \mathbf{q} .

Fig. 4 demonstrates how the Queue-stable region \mathcal{S}_Q and the All-saturated region \mathcal{S}_S vary with the transmission probability on each channel $q^{(c)}$, where $c \in \{1, \dots, L\}$. Without loss of generality, we set the numbers of channels $L = 2$, and

Algorithm 2: Determination of the Stability Status of Group M

Input: $n, \lambda, L, \mathbf{G} = (G_1, \dots, G_L)$, and $\mathbf{q} = (q^{(1)}, \dots, q^{(L)})$.

Output: $(n, \lambda, \mathbf{q}, \mathbf{G}) \in \{\mathcal{S}_Q, \mathcal{S}_S\}$

```

1 Calculate  $\lambda_{\max}$  in Eq. (12).
2 if  $\lambda < \lambda_{\max}$  then
3   for  $c = 1, 2, \dots, L$  do
4     Calculate  $q_{LB}^{(c)}$  and  $q_{UB}^{(c)}$  in Eq. (8) and (9);
5     Calculate  $\lambda_B^{(c)}$  in Eq. (11);
6     if  $\lambda \geq \lambda_B^{(c)}$  or  $q^{(c)} \notin [q_{LB}^{(c)}, q_{UB}^{(c)}]$  then
7        $(n, \lambda, \mathbf{q}, \mathbf{G}) \in \mathcal{S}_S$ ;
8       break;
9     end
10  end
11   $(n, \lambda, \mathbf{q}, \mathbf{G}) \in \mathcal{S}_Q$ ;
12 else
13    $(n, \lambda, \mathbf{q}, \mathbf{G}) \in \mathcal{S}_S$ ;
14 end

```

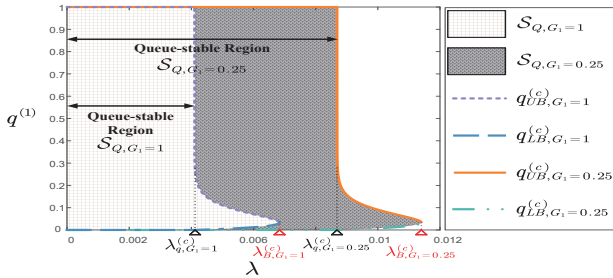


Fig. 5. Queue-stable region \mathcal{S}_Q versus the packet arrival rate λ of queues from MLDs. $L = 2, G_2 = 1.5, G_1 \in \{0.25, 1\}, q^{(2)} = 0.05, n = 30$.

derive the boundaries $q_{LB}^{(2)}$ and $q_{UB}^{(2)}$ on channel 2. Note that this process is symmetric, and we can also use $q^{(2)}$ to obtain $q_{LB}^{(1)}$ and $q_{UB}^{(1)}$. It can be observed from Fig. 4 that the shape of the Queue-stable region \mathcal{S}_Q shrinks as the traffic from the external network becomes intensive. For instance, with $G_1 = 1$ and $G_2 = 1.5$, \mathcal{S}_Q is a small ellipse in Fig. 4b. On the other hand, \mathcal{S}_Q enlarges significantly if $G_1 = 0.5$ and $G_2 = 0.25$. Intuitively, with light traffic from the external network, there is more freedom on the selection of \mathbf{q} that can guarantee a stable queue, where Group M is unsaturated. Similar observation can also be obtained in Fig. 5, which demonstrates how the Queue-stable region \mathcal{S}_Q varies with the input rate λ . In particular, with $\lambda \in (0, \lambda_q^{(c)}]$, the boundaries of the Queue-stable region satisfy $q_{LB}^{(c)} = 0$ and $q_{UB}^{(c)} = 1$, which conforms to the first terms in (8) and (9). On the other hand, with $\lambda \in (\lambda_q^{(c)}, \lambda_B^{(c)})$, as λ increases, \mathcal{S}_Q shrinks and then vanishes when $\lambda \geq \lambda_{B,G_c}^{(c)}$.

V. OPTIMIZATION OF MEAN ACCESS DELAY

Note that with *Cloning* strategy, each MLD sends a full copy of each packet among different channels, improving the reliability and reducing the delay, which is promising for IoT applications with ultra-reliable low-latency communication requirements. Regarding this, this paper investigates the delay performance limit of multi-link group and addresses how to

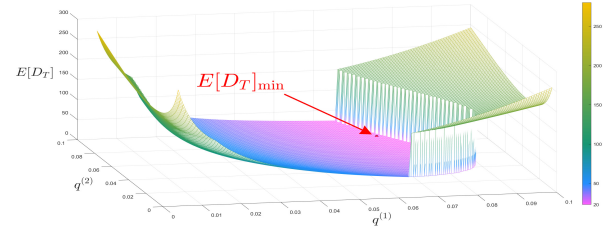


Fig. 6. Mean access delay of all the MLDs $E[D_T]$ versus the transmission probabilities on channel 1 and channel 2, i.e. $q^{(1)}$ and $q^{(2)}$. $L = 2, G_2 = 0.5, G_1 = 1.5, \lambda = 0.2/n, n = 30$.

properly tune the transmission probability $q^{(c)}$ on each channel c to achieve such performance limit.

Let D_i denote the time spent from State $i \in \{0, T\}$ to the transmission completion, and Y_0 as the sojourn time of a HoL packet in State 0. Combining the discrete-time Markov chain presented in Fig. 2 and [9], we have

$$D_T = \begin{cases} 1, & \text{with probability } \pi_T \\ 1 + D_0, & \text{with probability } 1 - \pi_T, \end{cases} \quad (13)$$

and $D_0 = Y_0$. Note that D_T is the service time of HoL packets which is also the access delay. By following our proceeding analysis in [1], the mean access delay of the HoL packets from the MLDs, denoted as $E[D_T]$, can be obtained as

$$E[D_T] = \frac{1}{1 - \prod_{c=1}^L (1 - q^{(c)} p^{(c)})}, \quad (14)$$

which is determined by the MLDs' transmission probabilities \mathbf{q} and the steady-state successful transmission probabilities. We are interested in the following optimization

$$E[D_T]_{\min} = \min_{q^{(c)}, c \in \{1, \dots, L\}} E[D_T]. \quad (15)$$

The problem in (15) is a L -dimensional continuous-space optimization problem and transmission probabilities on all channels have to be collaboratively tuned. Also, the objective equation in (14) is implicit due to the bistable behavior of the network. Here we present a DE-based (Differential Evolution) method to obtain the approximate global optimal mean access delay $E[D_T]_{\min}$ and the corresponding random access strategy \mathbf{q}^* for the MLDs as presented in Algorithm 3. The proposed DE-based algorithm is different from the classic one as shown in lines 6 and 15-16, where Algorithm 1 and Algorithm 2 is jointly included to determine the queue status of all the MLDs. It is essential since the mean access delay performance is discontinuous between \mathcal{S}_Q and \mathcal{S}_S . The detailed explanation of Algorithm 3 is omitted due to the page limit.

The effectiveness of Algorithm 3 is verified by simulation results. Fig. 6 presents how the mean access delay $E[D_T]$ varies with the transmission probabilities on both channels when $L = 2$, i.e., $q^{(1)}$ and $q^{(2)}$. The optimal access strategy derived from Algorithm 3 is $\mathbf{q}^* = (0.0746, 0.0722)$, from which the global optimal mean access delay $E[D_T]_{\min} \approx 23.17$ slots, as shown in Fig. 6. Compared to single-link slotted Aloha networks, where the mean access delay can exceed hundreds of time slots [14], MLD demonstrates its great potential in improving the access delay performance, even though one of the channels occurs intense contention (e.g. $G_1 = 1.5$).

Algorithm 3: DE Algorithm for Globe Mean Access Delay Minimization

Input: $n, \lambda, L, \text{iternum}, \text{popnum}, CR, F, q_{\min}, q_{\max}, \mathbf{G} = (G_1, \dots, G_L)$.

Output: $\mathbf{q}^* = (q^{(1)*}, \dots, q^{(L)*}), E[D_T]_{\min}$.

```

1  $E[D_T]_{\min} \leftarrow \infty$ ;
2 for each particle  $i \leftarrow 1$  to  $\text{popnum}$  do
3   for each channel  $c \leftarrow 1$  to  $L$  do
4     Initialize position  $q_{i,0}^{(c)} \in [q_{\min}, q_{\max}]$ ;
5   end
6   Calculate  $E[D_T]_{i,0}$  with (4), (14) and Algorithm 1;
7 end
8 for Iteration  $t \leftarrow 1$  to  $\text{iternum}$  do
9   for each particle  $i = 1$  to  $\text{popnum}$  do
10    for  $c \leftarrow 1$  to  $L$  do
11       $m_{i,t}^{(c)} = q_{r1,t-1}^{(c)} + F \cdot (q_{r2,t-1}^{(c)} - q_{r1,t-1}^{(c)})$ ,
12       $\forall r1, r2, r3 \in \text{popnum}, i \neq r1 \neq r2 \neq r3$ ;
13       $q_{i,t}^{(c)} = q_{i,t-1}^{(c)}$ ;
14      if  $\text{rand}(0, 1) \leq CR$  then  $q_{i,t}^{(c)} = m_{i,t}^{(c)}$ ;
15    end
16    Determine the queue status with Algorithm 2;
17    Calculate  $E[D_T]_{i,t}$  with  $\mathbf{q}_{i,t} = (q_{i,t}^{(1)}, \dots, q_{i,t}^{(L)})$ 
18    according to (4), (14) and Algorithm 1;
19    if  $E[D_T]_{i,t} > E[D_T]_{i,t-1}$  then
20       $E[D_T]_{i,t} = E[D_T]_{i,t-1}$ ;  $\mathbf{q}_{i,t} = \mathbf{q}_{i,t-1}$ ;
21    end
22     $E[D_T]_t = \min\{E[D_T]_{1,t}, \dots, E[D_T]_{\text{popnum},t}\}$ ;
23     $\mathbf{q}_t = \arg \min\{E[D_T]_{1,t}, \dots, E[D_T]_{\text{popnum},t}\}$ ;
24    if  $E[D_T]_t < E[D_T]_{\min}$  then
25       $E[D_T]_{\min} = E[D_T]_t$ ;  $\mathbf{q}^* = \mathbf{q}_t$ ;
26  end

```

VI. CONCLUSION

In this paper, we develop an analytical model for multi-link slotted Aloha with *Cloning* strategy. The steady-state points in different channels and the boundaries between different queue-status regions are derived, fostering a deep understanding of the interdependencies between steady-state points across individual channels. The mean access delay performance of the MLDs is also investigated and then derived through a heuristic algorithm. Our findings underscore that the saturation status of each MLD is intrinsically tied to various factors including packet arrival rate, channel access strategy, and the channel contention processes of all channels. The intensive contention in any of the channels exerts influence on the stability region of MLDs and their random access strategies on other channels and eventually affects the access delay performance.

APPENDIX A PROOF OF THEOREM 1

From Lemma 1, the local maximum service rate of the MLDs' data queues $\pi_{T,local}^{(c)}$ can be derived at $q^{(c)} = \frac{1}{n}$ when

operating in \mathcal{S}_S , which can be given by

$$\pi_{T,local}^{(c)} = 1 - \frac{n \exp(1+G_c) - 1}{n \exp(1+G_c)} \cdot \prod_{i \in L \setminus c} \frac{\exp(nq^{(i)} + G_i) - q^{(i)}}{\exp(nq^{(i)} + G_i)}. \quad (16)$$

Combining Eq. (3), (12) and (16), we can conclude that if $\pi_{T,local}^{(c)} \leq \lambda$ holds, MLDs maintain in \mathcal{S}_S regardless of $q^{(c)}$ and we have the sufficient and necessary condition in Eq. (11).

However, if $\lambda \leq \lambda_q^{(c)}$ is not satisfied, we have $\lambda > \pi_T|_{q^{(c)}=0}$ and $\lambda < \pi_T|_{q^{(c)}=\frac{1}{n}}$ combining Eq. (12). As π_T monotonically increases as $q^{(c)} \in (0, \frac{1}{n})$ increases, combining Eq. (4) and (5), we have the second term in Eq. (8). As for $q^{(c)} \in (\frac{1}{n}, 1)$, since π_T decreases as $q^{(c)}$ increases within \mathcal{S}_S , if the condition

$$\prod_{i \in L \setminus c} \left[1 - \frac{q^{(i)}}{\exp(nq^{(i)} + G_i)} \right] \leq \frac{1-\lambda}{1-\exp(-n-G_c)}, \quad (17)$$

always holds, we have $\lambda \leq \pi_T|_{q^{(c)}=1}$ and thus the upper boundary of \mathcal{S}_Q is $q_{UB}^{(c)} = 1$ in the first term of Eq. (9) and from which we can derive Eq. (10). Otherwise, if $\lambda > \pi_T|_{q^{(c)}=1}$ is satisfied, there is only one root for $\pi_T = \lambda$ for $q^{(c)}$ in $(\frac{1}{n}, 1)$ and presents as the second term of Eq. (9).

REFERENCES

- [1] Y. Li, W. Zhan and L. Dai, "Rate-Constrained Delay Optimization for Slotted Aloha," *IEEE Trans. on Commun.*, vol. 69, no. 8, pp. 5283-5298, Aug. 2021.
- [2] S. Naribole, S. Kandala and A. Ranganath, "Multi-channel mobile access point in next-generation IEEE 802.11be WLANs," in *Proc. IEEE ICC*, Montreal, QC, Canada, pp. 1-7, Jun. 2021.
- [3] T. Song and T. Kim, "Performance analysis of synchronous multi-radio multi-link MAC protocols in IEEE 802.11 be extremely high throughput WLANs," *Appl. Sci.*, vol. 11, no. 1, pp. 317, 2021.
- [4] N. Korolev, I. Levitsky and E. Khorov, "Analytical Model of Multi-Link Operation in Saturated Heterogeneous Wi-Fi 7 Networks," *IEEE Wireless Commun. Lett.*, vol. 11, no. 12, pp. 2546-2549, Dec. 2022.
- [5] R. V. da Silva, J. Choi, J. Park, G. Brante and R. D. Souza, "Multichannel ALOHA Optimization for Federated Learning With Multiple Models," *IEEE Wireless Commun. Lett.*, vol. 11, no. 10, pp. 2180-2184, Oct. 2022.
- [6] N. Jiang, Y. Deng and A. Nallanathan, "Traffic Prediction and Random Access Control Optimization: Learning and Non-Learning-Based Approaches," *IEEE Commun. Mag.*, vol. 59, no. 3, pp. 16-22, Mar. 2021.
- [7] S. Yeh, S. Talwar, G. Wu, N. Himayat and K. Johansson, "Capacity and coverage enhancement in heterogeneous networks," *IEEE Wireless Commun.*, vol. 18, no. 3, pp. 32-38, Jun. 2011.
- [8] S. H. Chae, T. Kim and J. Hong, "Distributed Multi-Radio Access Control for Decentralized OFDMA Multi-RAT Wireless Networks," *IEEE Commun. Lett.*, vol. 25, no. 4, pp. 1303-1307, Apr. 2021.
- [9] L. Dai, "A Theoretical Framework for Random Access: Stability Regions and Transmission Control," *IEEE/ACM Trans. on Netw.*, vol. 30, no. 5, pp. 2173-2200, Oct. 2022.
- [10] J. Seo, B. Jung and H. Jin, "Modeling and Online Adaptation of ALOHA for Low-Power Wide-Area Networks (LPWANs)," *IEEE Internet Things J.*, vol. 8, no. 20, pp. 15608-15619, Oct.15, 2021.
- [11] H. Huang, T. Ye, T. T. Lee and W. Sun, "Delay and Stability Analysis of Connection-Based Slotted-Aloha," *IEEE/ACM Trans. Netw.*, vol. 29, no. 1, pp. 203-219, Feb. 2021.
- [12] J. J. Nielsen, R. Liu and P. Popovski, "Ultra-Reliable Low Latency Communication Using Interface Diversity," *IEEE Trans. on Commun.*, vol. 66, no. 3, pp. 1322-1334, March 2018.
- [13] L. Kleinrock and F. Tobagi, "Packet Switching in Radio Channels: Part I - Carrier Sense Multiple-Access Modes and Their Throughput-Delay Characteristics," in *IEEE Trans. on Commu.*, vol. 23, no. 12, pp. 1400-1416, Dec. 1975.
- [14] W. Zhan and L. Dai, "Access Delay Optimization of M2M Communications in LTE Networks," *IEEE Wireless Commun. Lett.*, vol. 8, no. 6, pp. 1675-1678, Dec. 2019.